Electronic Supplementary Material (ESI) for Energy & Environmental Science.

Supplementary information for: In-line, roll-to-roll morphology analysis of organic solar cell active layers

Lea H. Rossander, Henrik F. Dam, Jon E. Carlé, Martin Helgesen, Ivan Rajkovic, Michael Corazza and Frederik C. Krebs and Jens W. Andreasen*

CALCULATION OF THE TOTAL SCANNED VOLUME

The constant wet thickness experiments had four different dry thickness T of the polymer/fullerene films of 964 nm, 723 nm, 482 nm and 241 nm. Therefore the total scanned volume for each of those experiments amounts to

$$V = t_{scan} * v * T * W = 1\,min * \frac{0,5\,m}{min} * 482\,nm * (2 + 1,5 + 1 + 0,5) * 13\,mm$$

$$= 1,446 * 10^{-8} m^3 = 14,46\,mm^3,$$

with a nearly constant width $W = 13mm$ and web speed $v = 0,5\frac{m}{min}$.

We performed 4 of those experiments for the wide angle measurements, as well as 2 of these for the small angle measurements. This gives a total scanned dry-volume counting all experiments of

$V_{tot} = 15,665mm^3 * 6 = 93,990mm^3$

CALCULATION OF THE SCANNED DRYING TIME

As the measurements were performed while the coater head was moving along the foil, the relative speed of head and foil determined the probed drying time. The foil speed was constant at 500mm/min and the coater head moved 140mm in one minute, giving it a speed of $\frac{140\,mm}{60\,sec} * \frac{60\,sec}{min} = 140\frac{mm}{min}$

We are interested in maximizing the time-resolution and therefore choose the data where the head moved in the same direction as the moving film, resulting in a reduced relative speed of 361 mm/min (=500-139 mm/min). It is now simple to calculate the drying time probed by one of these measurements. The maximum distance between beam and head was 140 mm (l_2) and the minimal was 1mm(l_1), the drying time with the relative speed of 361 mm/min is then given by

$$t_{frame\_begin} = \frac{l_1}{v} * 60\frac{sec}{min} = 0,17\,sec$$

And in the final frame

$$t_{frame\_end} = \frac{l_2}{v} * 60\frac{sec}{min} = 23,27\,sec$$

WIDE ANGLE SCATTERING RESULTS:

The recorded wide angle scattering shows a clear out of plane peak appearing as the film dries, at approximately the expected position for P3HT. In order to attain a complete image of what the measurements showed, we analysed both the intensity distribution as a function of out of plane scattering angle q, and as a function of the azimuthal angle theta. The development of the (100) peak in q, and its width, contain information about the stacking distance of the polymer back bones, as well as the average crystallite sizes. The distribution along the azimuthal angle theta has information about how structured the crystallites are, and is also interesting. The PBDTTTZ-4 polymer shows a structure peak at (100) similar to the one for P3HT but at a lower angle around $0{,}27\ \text{Å}^{-1}$, which shows that the PBDTTTZ-4 polymer also has semi-crystalline packing and that it is slightly wider than P3HT with a d-spacing of about 21,5 Å. By fitting the structure peak with a Gaussian function plus a linear background in each scan, and the plotting the extracted values as a function of time, curves such as those in Figure 2 are obtained.

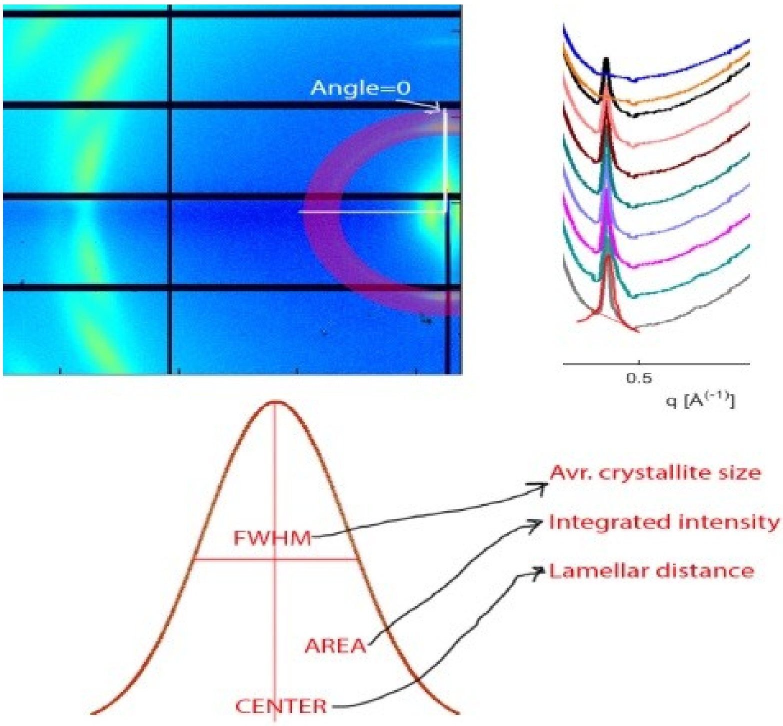

Figure 1 Explanatory graphic showing the procedure for producing the curves.

4-ZONE PLOTS – LAMELLAR DISTANCE, CRYSTALLITE SIZE, INTEGRATED INTENSITY AND ORIENTATION FACTOR

Using the technique described above, the following 4-part plots were generated for each mixture.

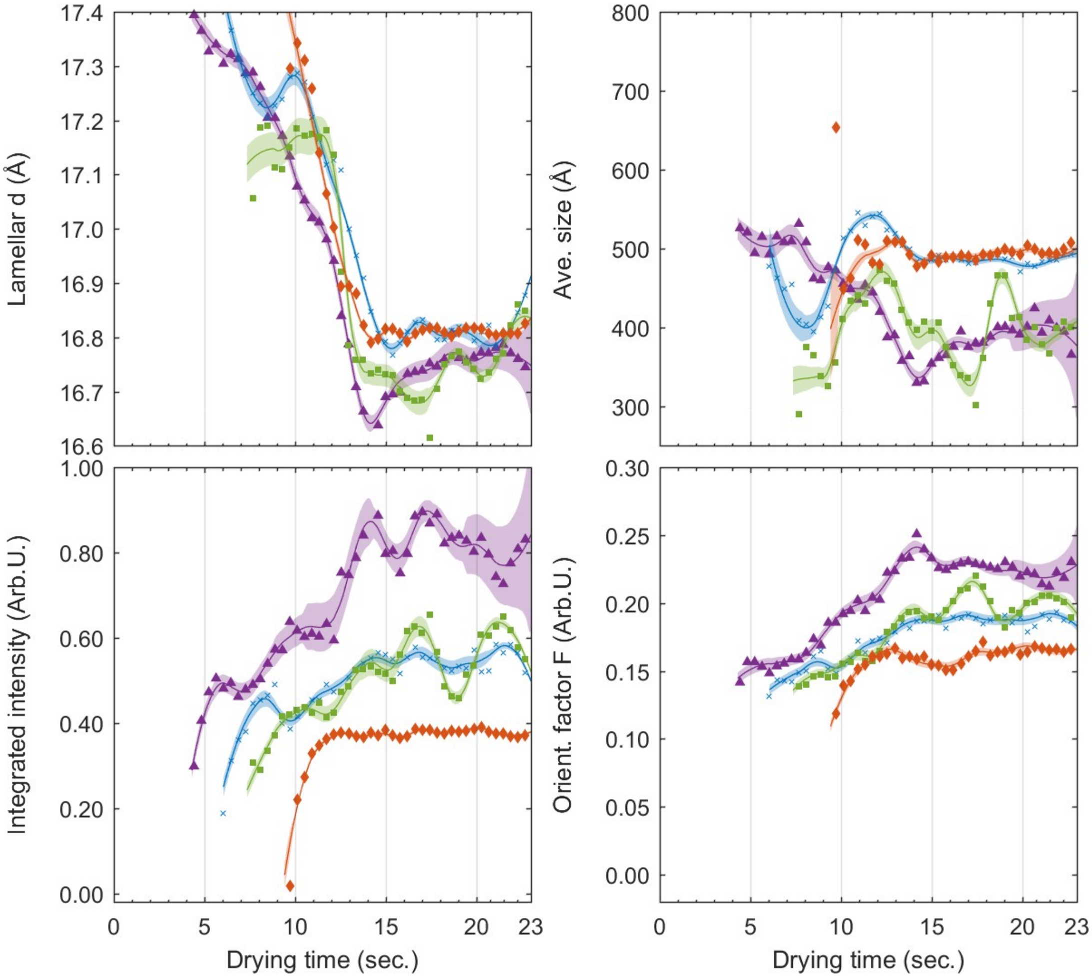

Figure 2 Plot showing the development of lamellar distance, average crystallite size, integrated intensity in the structure peak and order factor for pure P3HT. Concentrations: Purple=40:40, Blue=30:30, Green=20:20, Orange=10:10 P3HT.

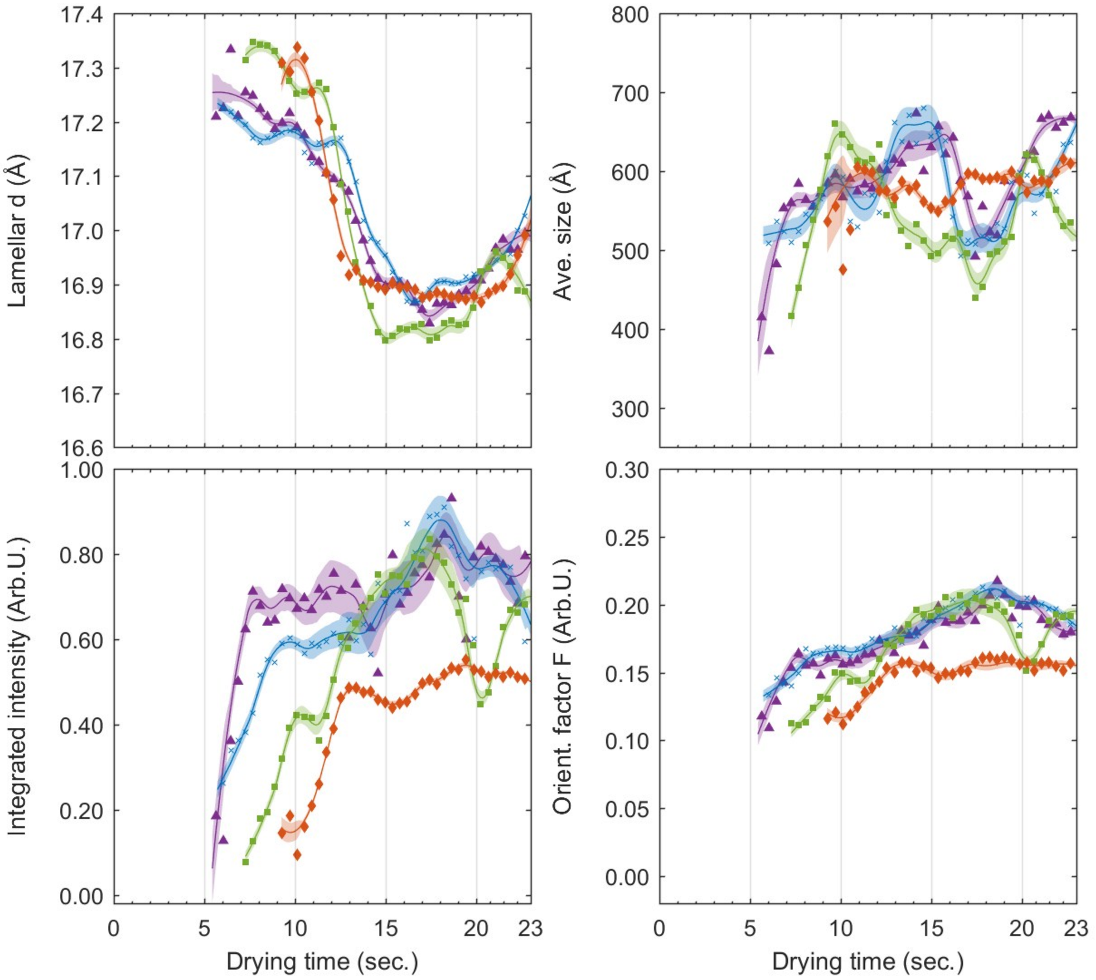

Figure 3 Plot showing the development of lamellar distance, average crystallite size, integrated intensity in the structure peak and order factor for P3HT:PCBM. Concentrations: Purple=40:40, Blue=30:30, Green=20:20, Orange=10:10 P3HT:PCBM.

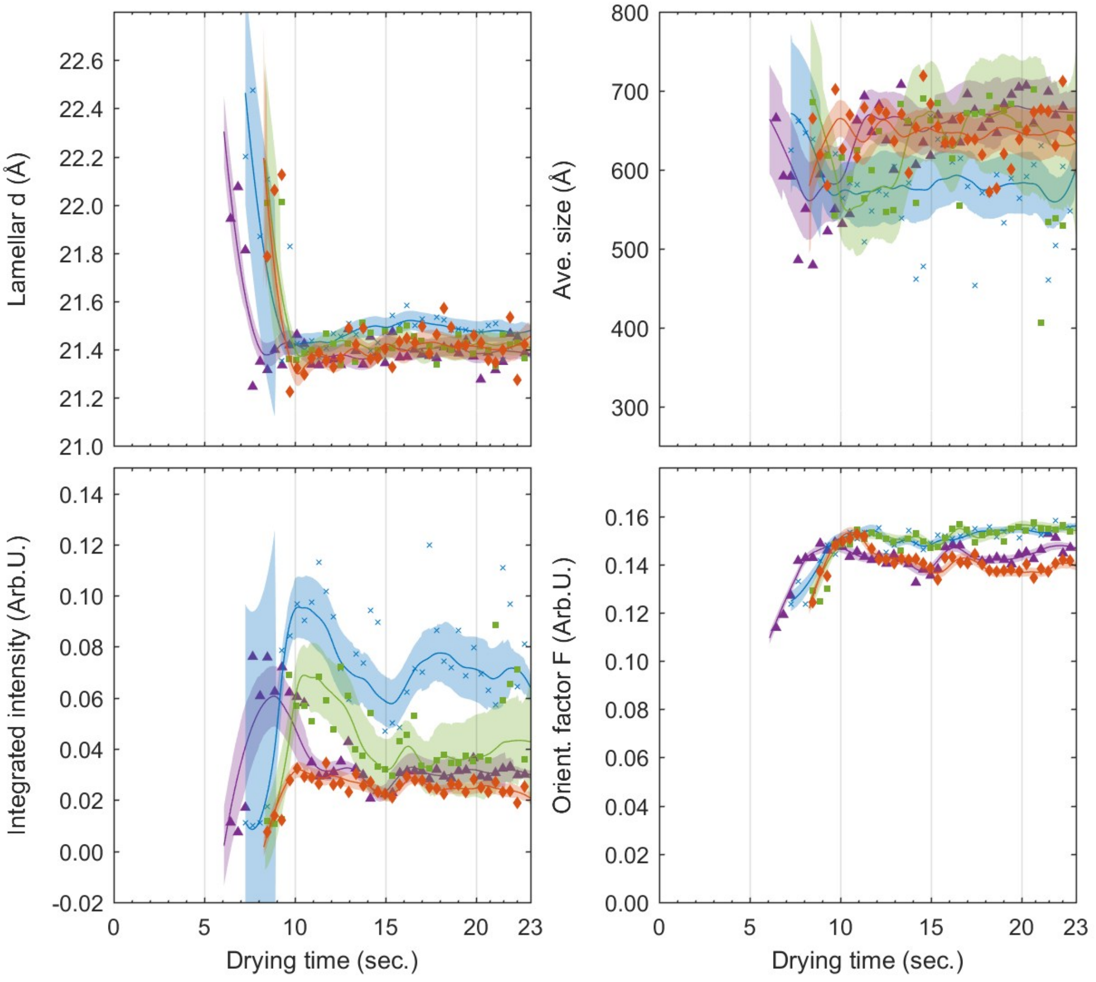

Figure 4 Plot showing the development of lamellar distance, average crystallite size, integrated intensity in the structure peak and order factor for pure PBDTTTZ-4. Purple=16:24 mg/ml, Blue=12:18 mg/ml, Green=8:12 mg/ml, Orange=4:6 mg/ml PBDTTTZ-4.

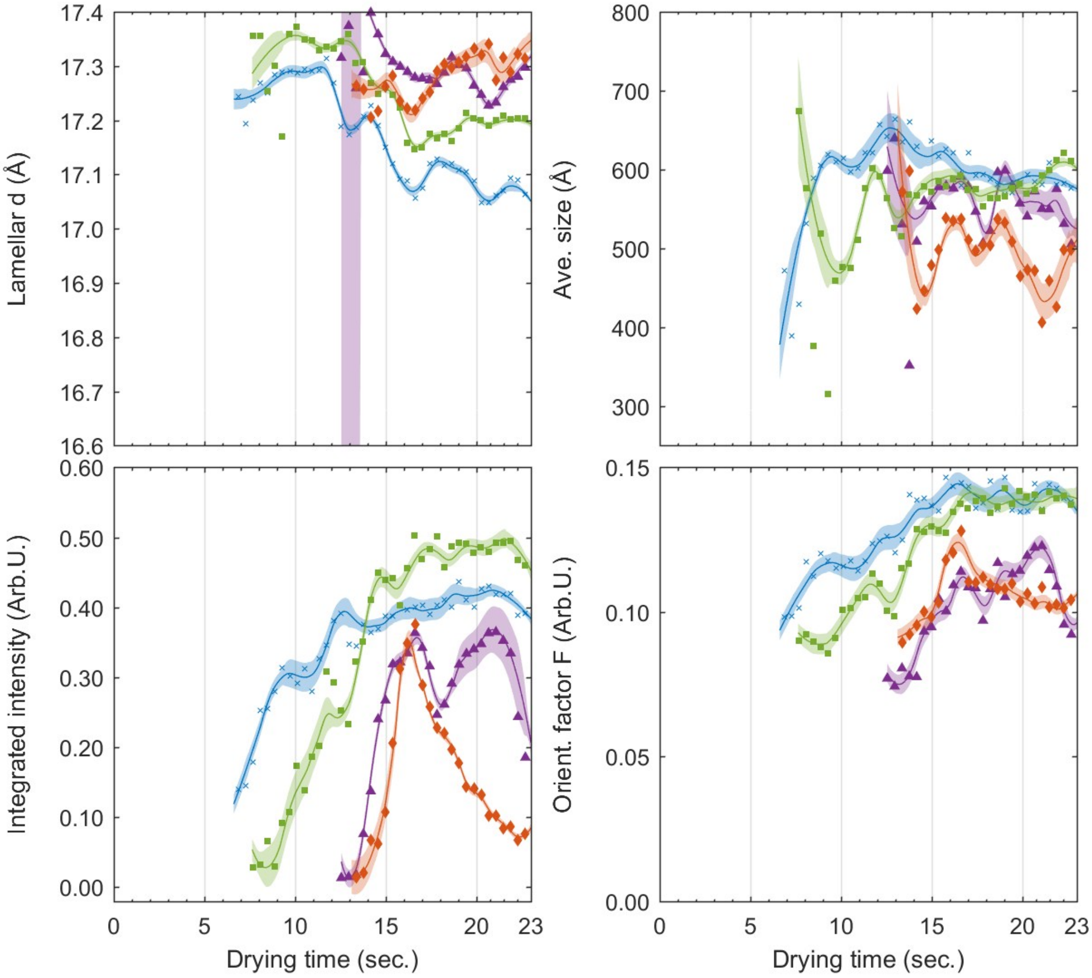

Figure 5 Plot showing the development of lamellar distance, average crystallite size, integrated intensity in the structure peak and order factor for P3HT:PCBM with constant dry thickness. Concentrations: Purple=40:40, Blue=30:30, Green=20:20, Orange=10:10 P3HT:PCBM.

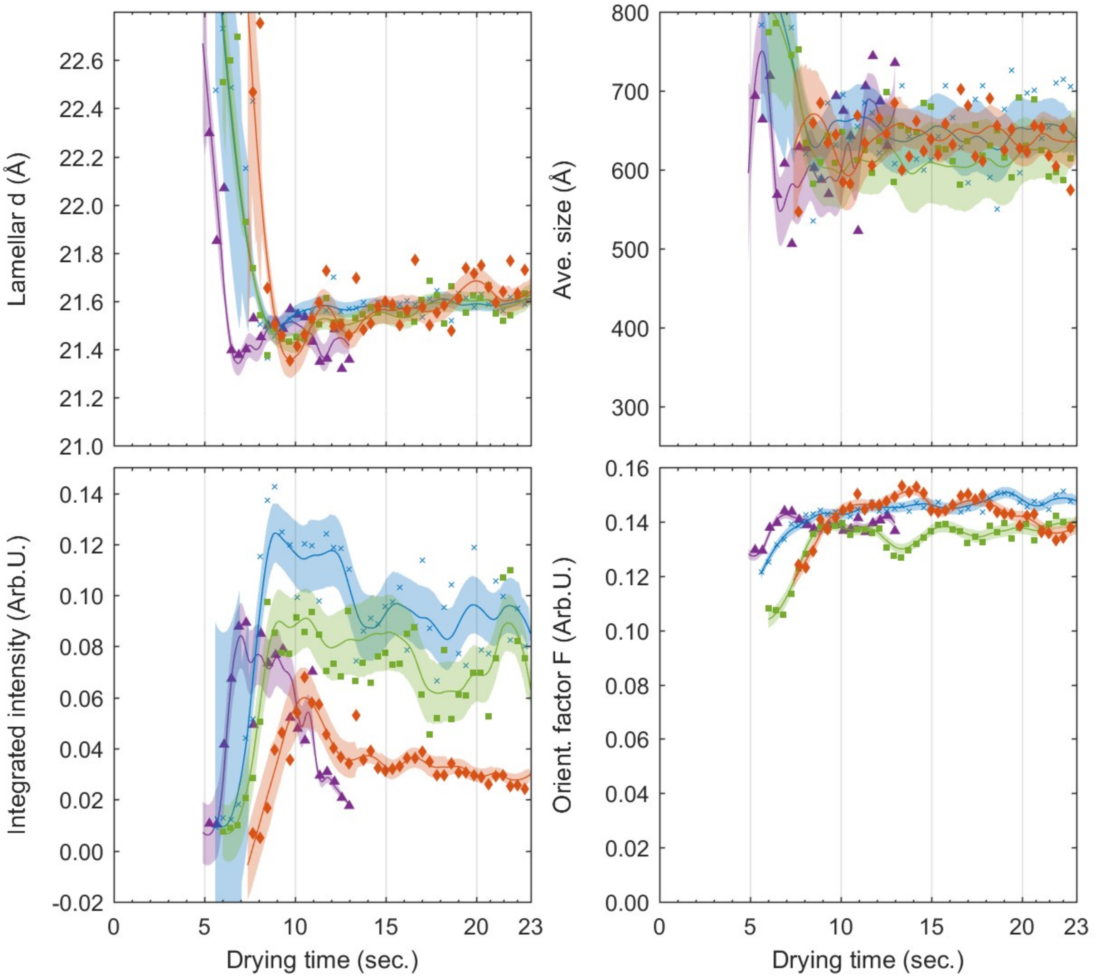

Figure 6 Plot showing the development of lamellar distance, average crystallite size, integrated intensity in the structure peak and order factor for PBDTTTZ-4:PCBM. Purple=16:24 mg/ml, Blue=12:18 mg/ml, Green=8:12 mg/ml, Orange=4:6 mg/ml PBDTTTZ-4:PCBM

INTENSITY VARIATIONS

The integrated intensity shows more variability for datasets where overall integrated intensity is high. At various points in the curves for integrated intensity, a second peak appears and disappears erratically, see Figure 7. This is an effect of multiple scattering events depending on X-ray incidence angle.

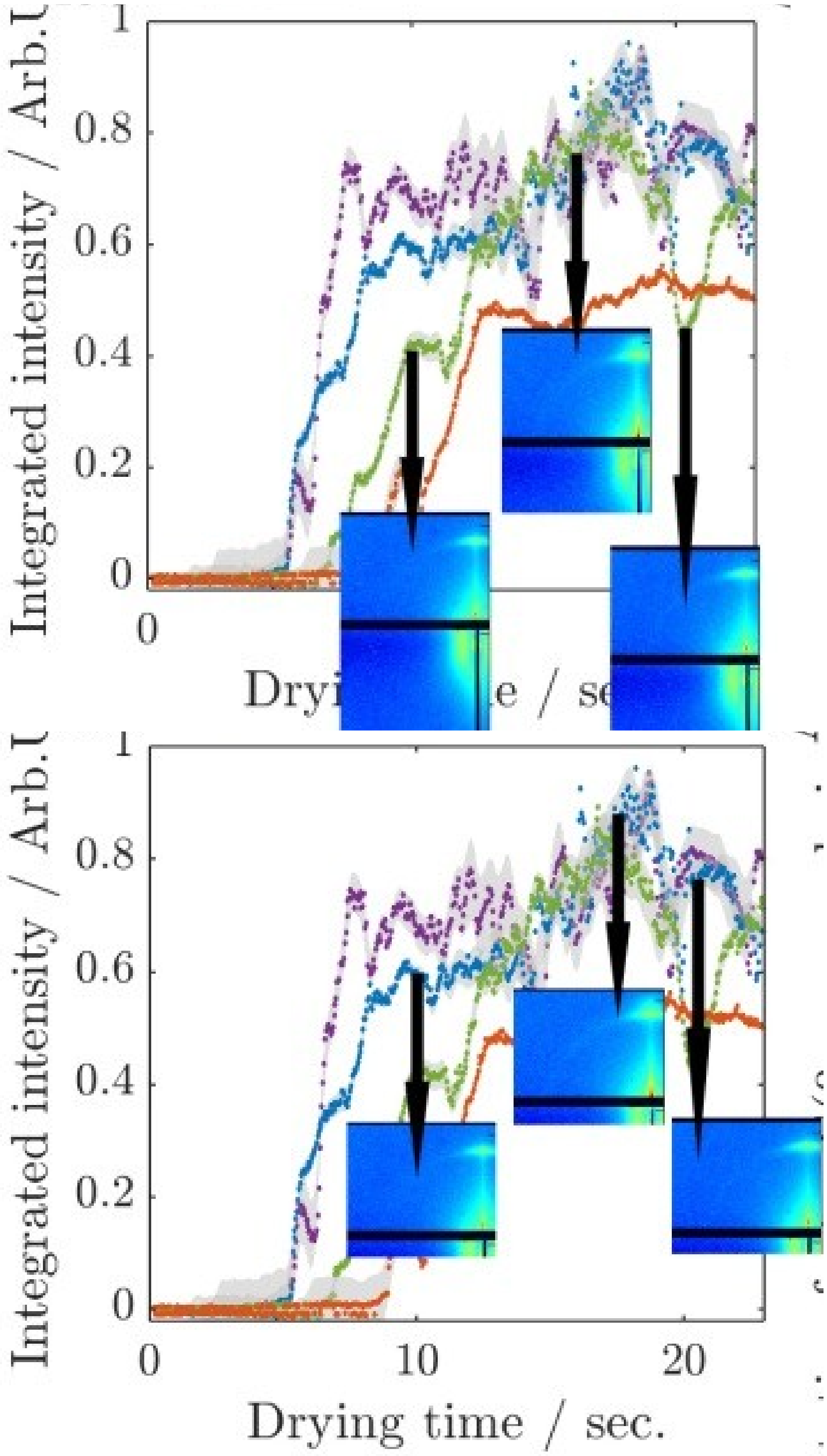

Figure 7 Two plots with 2D data inserted at highs and lows for the integrated intensity, for the second and third concentrations of P3HT:PCBM.

SOLVENT EVAPORATION

The change of the intensity of the PET background signal is an indirect indicator of the solvent evaporation, and it is plotted in Figure 8 and Fig. 9 as a function of drying time.

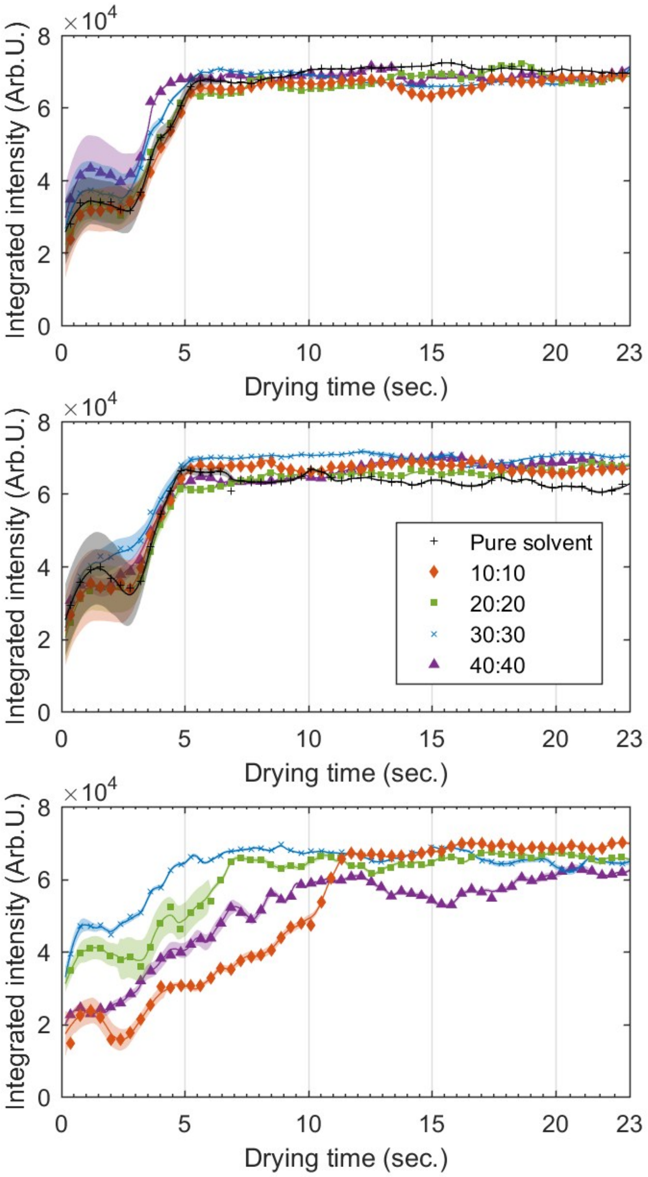

Figure 8 Plot showing the development of integrated counts in the PET region(q=0.4-3). The five concentrations showed as in legend. The 3 datasets from top =P3HT; middle=P3HT:PCBM; bottom=P3HT:PCBM const. dry thickness.

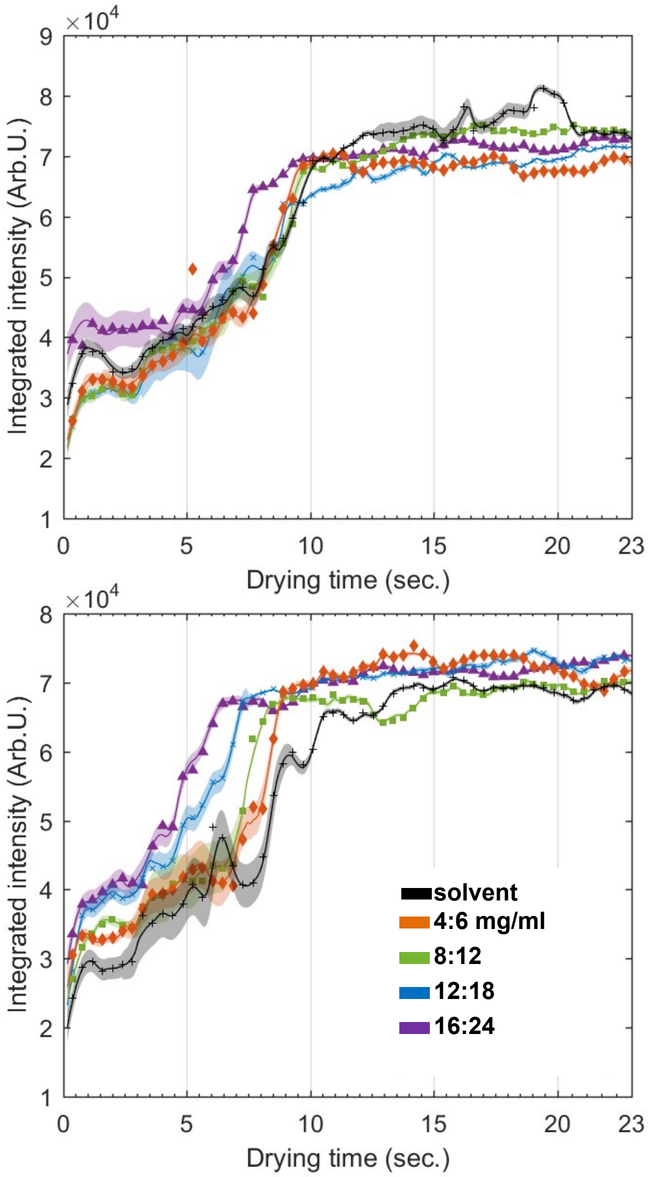

Figure 9 Plot showing the development of integrated counts in the PET region(q=0.4-3). The five concentrations showed as in legend. The 2 datasets from top=PBDTTTZ-4 and bottom=PBDTTTZ-4:PCBM.

ANNEALING MEASUREMENTS

The annealing experiments confirmed the observations made on short time scales, on longer time scales. The reduction in packing distance for P3HT and P3HT:PCBM was observed again. After establishing a good coat the foil was stopped on the heating plate while the scattering was measured for a period of time until it stopped changing. The PBDTTTz-4 measurement was run for much longer than the P3HT one because it was less known how the new polymer would behave. As the film was drying on a heating plate, this results in a combination of effects – both the evaporation of the solvent, but also a subsequent annealing due to the constant heat on the samples.

The measurements from the two experiments show that the crystallite sizes had not reached equilibrium in the short timescale measurements – the size observed for P3HT in the short timescale experiments reached around 600 Å, where in contrast, the equilibrium size reached in the long timescale annealing experiment was 400 Å. The P3HT crystallite size was also observed to reduce with annealing, until it stabilized after about 200 seconds in conjunction with a reduction in lamellar separation.

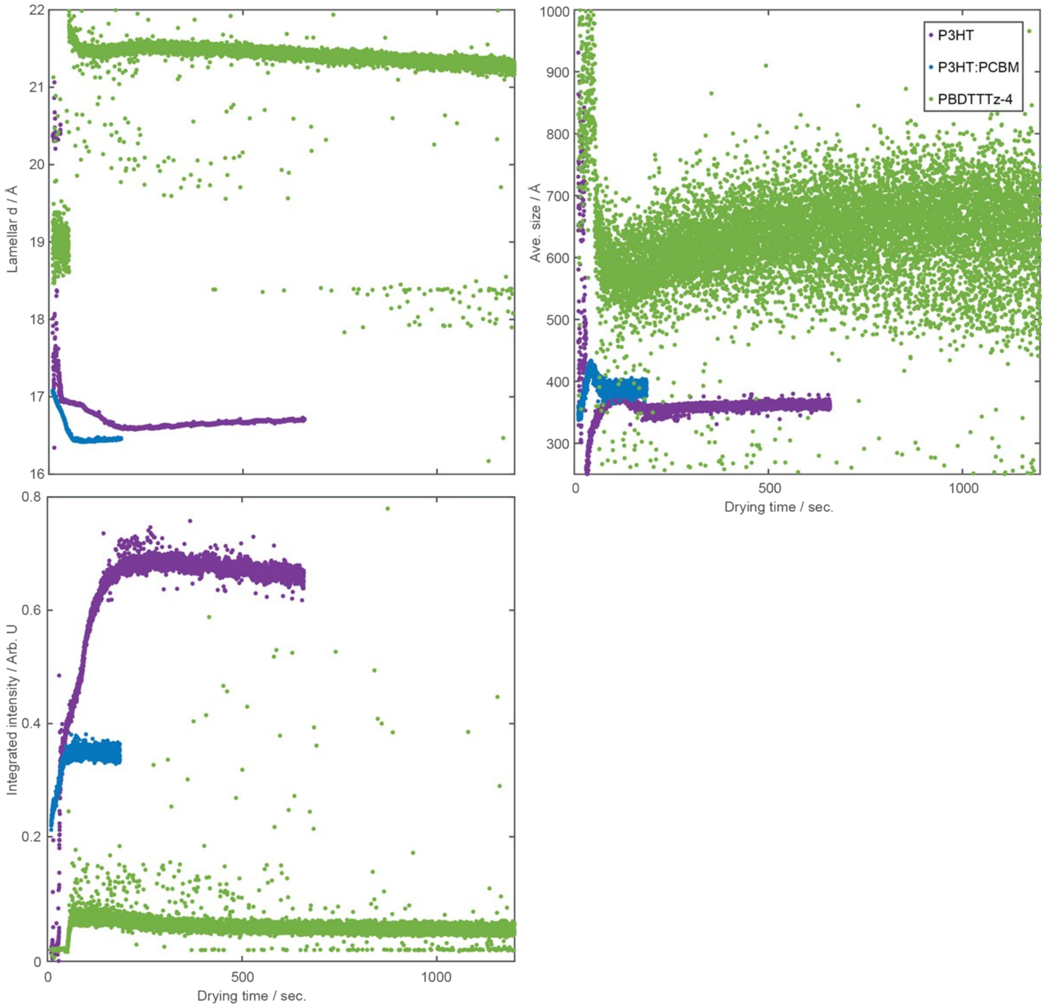

Figure 10 Plot showing the development of lamellar distance, average crystallite size and integrated intensity in the structure peak for the annealing measurements of P3HT, P3HT:PCBM and PBDTTTz-4:PCBM. As the film was drying on a heating plate, this results in a combination of effects – both the evaporation of the solvent, but also a subsequent annealing due to the constant heat on the samples.

SMALL ANGLE SCATTERING

WATERFALL PLOTS:

The first analysis of the small angle scattering is based on waterfall plots that enable an overview of how the scattering develops with time. The resulting plots are shown in the following subfigures of Figure 11. There are two datasets for each blend.

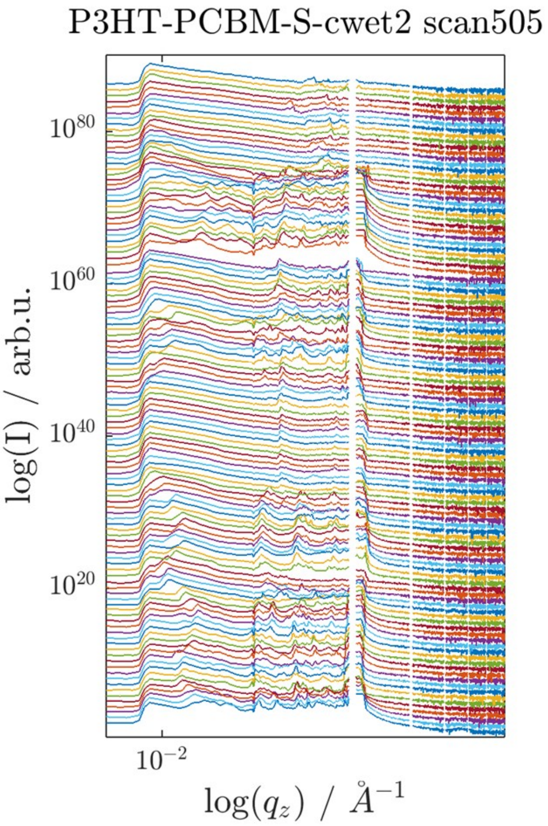
P3HT-PCBM-S-cwet2 scan505
10^{80}
10^{60}
10^{40}
10^{20}
$\log(I)$ / arb.u.
10^{-2}
$\log(q_z)$ / $\AA^{-1}$

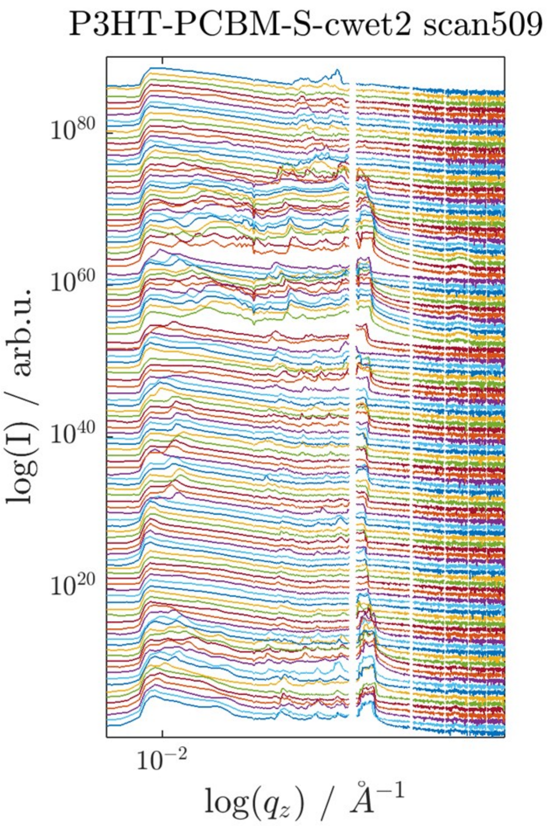
P3HT-PCBM-S-cwet2 scan509
10^{80}
10^{60}
10^{40}
10^{20}
$\log(I)$ / arb.u.
10^{-2}
$\log(q_z)$ / $\AA^{-1}$


0sek
Timeline
23,4sek

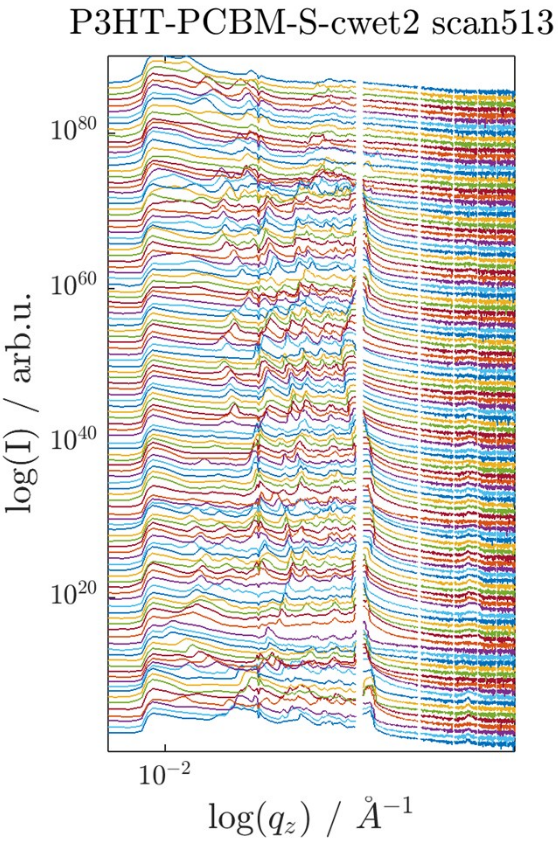
P3HT-PCBM-S-cwet2 scan513
10^{80}
10^{60}
10^{40}
10^{20}
$\log(I)$ / arb.u.
10^{-2}
$\log(q_z)$ / $\AA^{-1}$

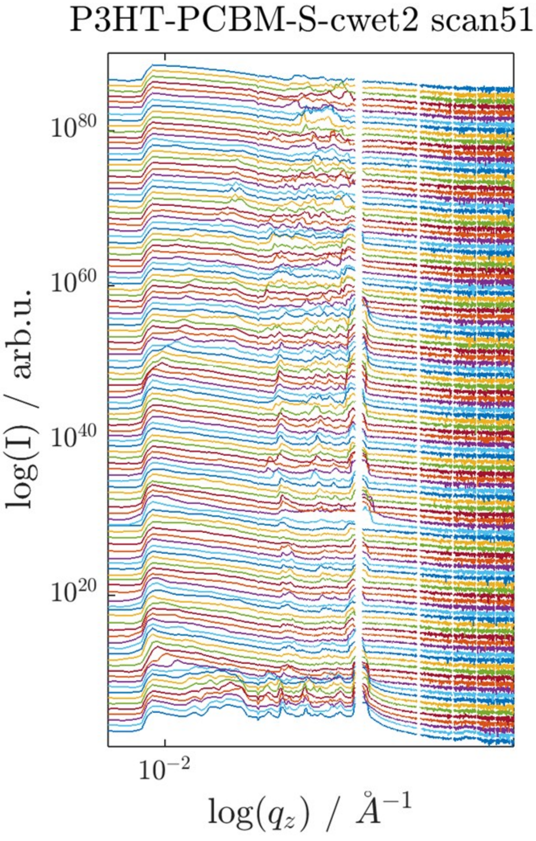
P3HT-PCBM-S-cwet2 scan517
10^{80}
10^{60}
10^{40}
10^{20}
$\log(I)$ / arb.u.
10^{-2}
$\log(q_z)$ / $\AA^{-1}$


0sek
Timeline
23,4sek

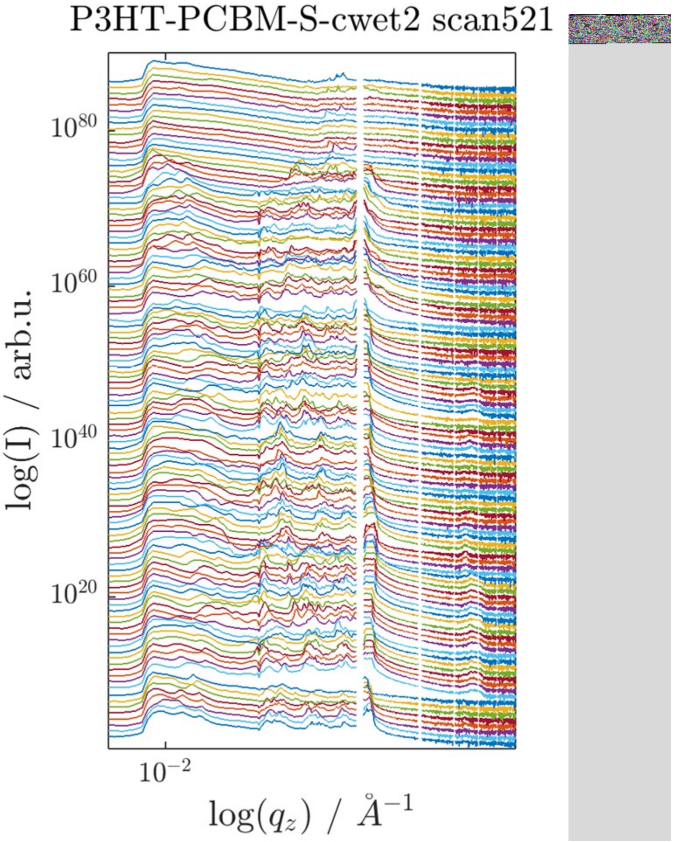

Figure 11 Waterfall-plot of line cuts through q=0 Line cuts for the second P3HT:PCBM measurement – from highest concentration(scan#505) to pure solvent (scan#521)

PICTURES OF THE SETUP AT THE BEAMLINE

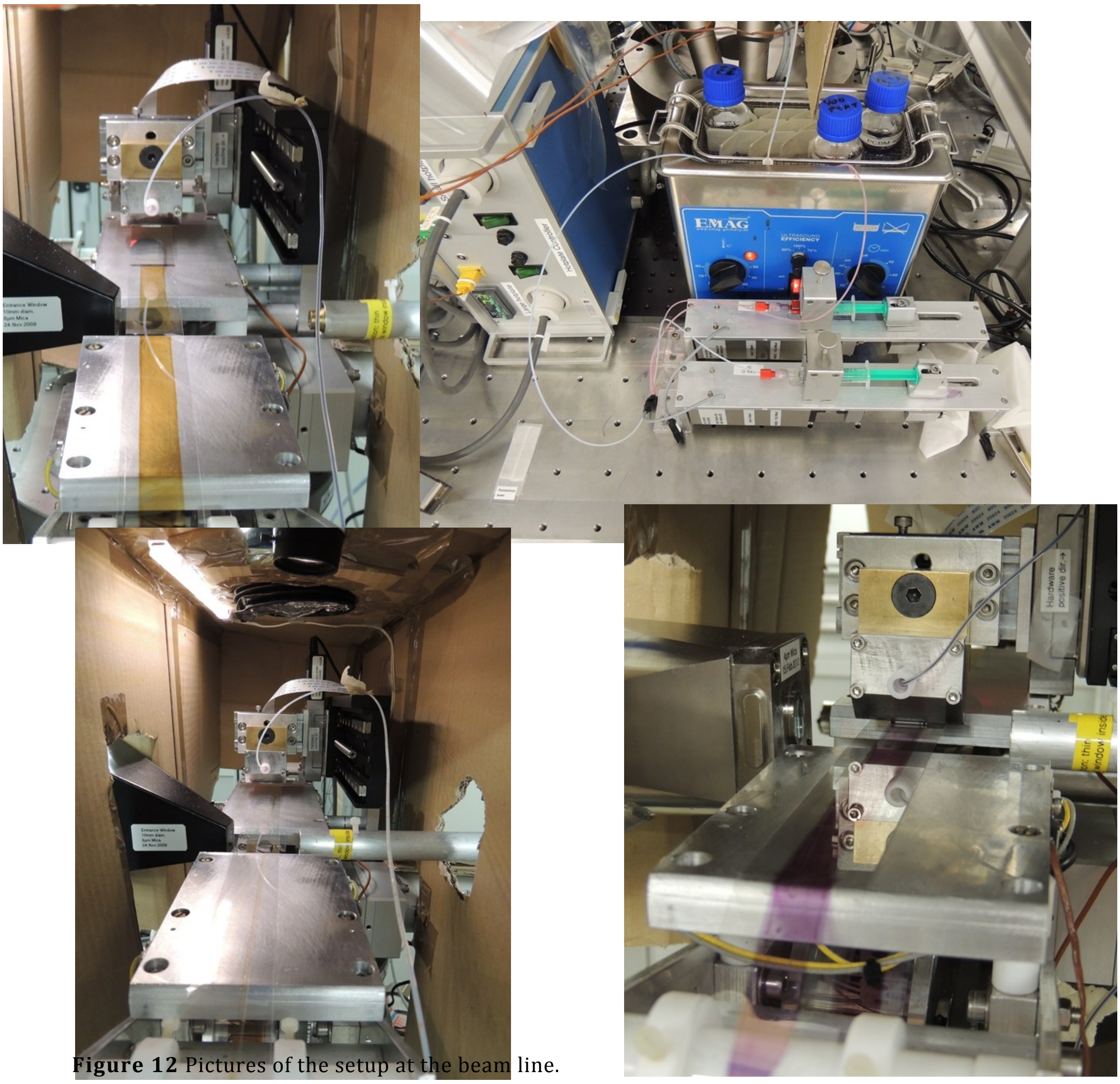

Figure 12 Pictures of the setup at the beam line.

CORRELATING COATING ANOMALIES WITH UNEXPLAINED OBSERVATIONS

Using the recorded real time images of the coat, we were able to explain all of the unexpected behaviour seen in both the dependence of the integrated intensity on time as well as on other parameters.

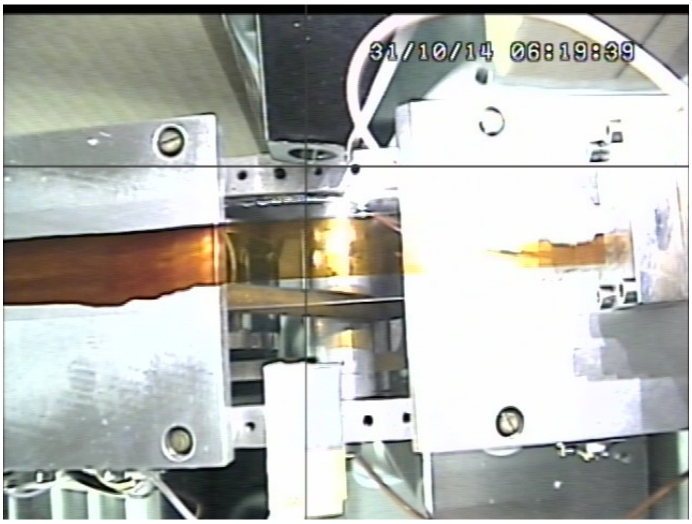

Figure 13 The coat clearly widens significantly at the corresponding time where the integrated intensity increases unexpectedly.

The correlation between the coat and the measurement is easier followed by watching the included video showing measurement and video feed of coat simultaneously.

MANUFACTURE OF SPIN COATED PBDTTTZ-4:PCBM SOLAR CELL AND J-V CHARACTERIZATION

Inverted photovoltaic devices were made by spin coating a ZnO precursor solution[1] onto precleaned, patterned indium tin oxide (ITO) glass substrates (9–15 Ω per square) (LumTec) followed by annealing at 140 °C for 10 min. The active layer was deposited by spin coating a 1:1.5 blend of the polymer and PCBM dissolved in 1,2-dichlorobenzene (30 mg ml^{-1}). After drying, this was followed by the application of PEDOT:PSS (Agfa EL-P 5010) diluted with isopropanol 2 : 1 (w/w) by spin-coating at 3000 rpm and then drying on a hotplate at 110 °C for 5 min. The device was completed by evaporation of silver as back electrode at 2–3 x 10^{-6} mbar. The active area of the cells was 0.25 cm^2. J–V characteristics were measured under AM1.5G corresponding to 100 mW cm^{-2} white light using a solar simulator from Steuernagel Lichttechnik.

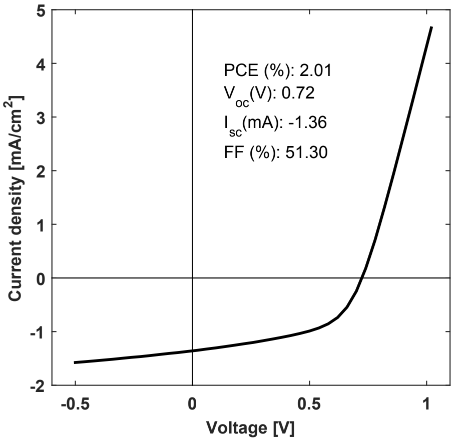

Figure 14 J-V characteristics of spin coated PBDTTTZ-4:PCBM device with an active area of 0.25 cm^2.

DIFFERENTIAL SCANNING CALORIMETRY (DSC)

DSC experiments were carried out with a Mettler Toledo TGA/DSC1 STAR System instrument at a heating rate of 10 °C/min under nitrogen. Sample size was about 8 mg, and polymers were used as obtained after Soxhlet extraction.

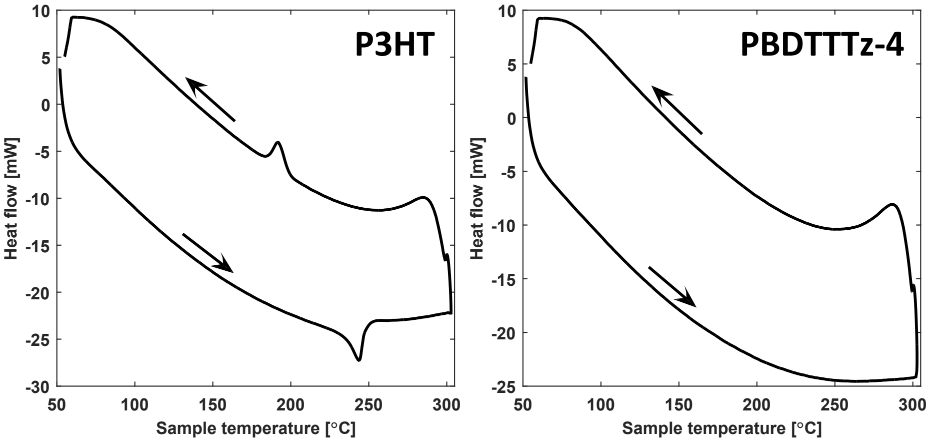

Figure 15 DSC traces of solid, neat polymers P3HT and PBDTTTz-4.

1. Sondergaard, R., Helgesen, M., Jorgensen, M. & Krebs, F. C. Fabrication of Polymer Solar Cells Using Aqueous Processing for All Layers Including the Metal Back Electrode. *Adv. Energy Mater.* **1,** 68–71 (2011).